Taylor & Francis
Taylor & Francis Group

RESEARCH ARTICLE

🔓 OPEN ACCESS ✅ Check for updates

Identification of a chromatin regulator signature and potential candidate drugs for primary open-angle glaucoma

Xinyue Zhang[a,b*], Lulu Xiao[a,c*], Xiaoyu Zhou[a], Jiahao Xu[a], Li Liao[b], Ping Wu[b], Zhimin Liao[a] and Xuanchu Duan 🄳[a,b]

[a]Glaucoma Institute, Hunan Engineering Research Center for Glaucoma with Artificial Intelligence in Diagnosis and Application of New Materials, Changsha Aier Eye Hospital, Changsha, Hunan, China; [b]Aier School of Ophthalmology, Central South University, Changsha, Hunan, China; [c]Aier Eye Hospital, Jinan University, Guangzhou, China

ABSTRACT
Aims: This research aims to establish a chromatin regulator (CR) signature to provide new epigenetic insights into the pathogenesis of primary open-angle glaucoma (POAG).
Materials & methods: The expression profile of CRs in trabecular meshwork (TM) tissues was analyzed by bioinformatics analysis; The selected hub CRs were further verified by cell experiments.
Results: We found the immune microenvironment of the TMwas changed in POAG patients and identified 3 differentially expressed CRs that were relevant to immunity. Then, we successfully constructed and proved a predicted signature based on these 3 CRs, which could effectively predict the risk of POAG. The genes co-expressed with these 3 CRs and miRNAs with are gulatory relationship were identified, and a miRNA-hub CR network was successfully constructed. The results of the Gene Set Enrichment analysis indicated that these 3 hub CRs were all associated with neurodegenerative diseases. Moreover, the human trabecular meshwork cell (HTMC) oxidative stress model was constructed, and KDM5B was significantly down-regulated in this cell model. Finally, we found 10 agents that might be helpful for patients with POAG.
Conclusions: Dysregulation of CR expression in TM tissues may be involved in the occurrence and progression of POAG through multiple mechanisms.

1. Introduction

Glaucoma is characterized by optic nerve damage with characteristic visual field impairment. It is estimated that more than 111 million people worldwide will suffer from glaucoma by the year 2040 [1]. According to statistics, glaucoma is the leading cause of irreversible vision impairment [2]. Notably, primary open-angle glaucoma (POAG) accounts for approximately 74% of glaucoma cases and is the most frequent type [1]. The risk factors for POAG include increasing age, increased intraocular pressure (IOP), and family history, of which IOP is the only modifiable risk factor in current studies [3]. The critically important factor affecting the level of IOP is whether the aqueous humor (AH) drainage is unobstructed. Under physiological conditions, the production and efflux of AH are in a state of dynamic balance, and the imbalance of dynamic balance often causes an increase in IOP. Moreover, 75% to 90% of the total AH in the human eye is discharged through the conventional pathway, also known as the trabecular meshwork (TM) pathway. Therefore, TM plays an essential regulatory role in AH drainage.

Human trabecular meshwork cells (HTMCs) perform two leading roles *in vivo*, including the secretion of specific enzymes and extracellular matrix (ECM) and the phagocytosis of debris in AH [4]. With the increase in age and the occurrence of eye diseases,

the apoptosis and senescence of HTMCs are accelerated [5–8]. The intracellular actin reticulum is cross-linked, and the ECM is abnormally accumulated [9,10], which obstructs the outflow of AH and ultimately leads to the increase of IOP [11]. The continuous rise of IOP induces the death of retinal ganglion cells (RGCs), resulting in irreversible vision loss. At present, the treatment methods for glaucoma include drugs, lasers, surgical treatment, etc. However, due to drug dependence, post-surgical scarring, and other conditions leading to the re-elevation of IOP, we urgently need to find new treatment methods. We considered that the treatment method to restore the number and function of HTMCs is the closest to restoring the AH circulation in a physiological state, which is more consistent with clinical needs in reducing IOP. This requires us to further understand the pathophysiological mechanism of TM in POAG.

The prevalence of first-degree relatives of POAG patients is 4 to 10 times that of the general population [12], indicating the correlation between genetic factors and this disease. However, studies have also shown that simple genetic patterns are not suitable for the identification of characteristic genes in POAG patients [13]. Rather, POAG susceptibility is influenced by the variation of multiple genes, environmental factors, and their interactions [14]. There is also growing evidence that epigenetic regulation appears to

---

Article highlights

- Dysregulation of chromatin regulator (CR) expression in trabecular meshwork (TM) tissues may be involved in the occurrence and progression of primary open-angle glaucoma (POAG).
- The immune microenvironment of the TM may be changed in POAG patients, and 3 differentially expressed CRs (RBBP7, CBX6,and KDM5B) were relevant to immunity.
- A predicted signature based on 3 CRs (RBBP7, CBX6, and KDM5B) was successfully constructed and proved, which could effectively predict the risk of POAG.
- KDM5Bwas significantly down-regulated in the human trabecular meshwork cells (HTMCs)oxidative stress cell model. KDM5B might be involved in cell damage during oxidative stress in the TM tissues.
- Uranium acetate CTD 00000229, URANIUM CTD00006964, fumonisin b1 CTD 00002395, 7646-79-9 CTD 00000928, METHOXYACETIC ACIDCTD 00000714, Promegestone CTD 00006626, hydrochloric acid, CTD 00006115,8-azaguanine HL60 DOWN, syrosingopine PC3 UP and harmine PC3 UP might be helpful for patients with POAG.

play an important role in glaucoma [15,16]. Therefore, studying epigenetic changes in POAG may provide many new clues to understanding disease occurrence. Most previous research focused on the overall acetylation or methylation level of the whole genome but did not identify specific loci or genes [17,18]. Thus, the epigenetic mechanisms and targeted therapeutic approaches in maintaining the AH outflow remain to be determined.

Chromatin regulators (CRs) are indispensable regulatory elements of epigenetics [19]. CRs are a group of closely related enzymes with unique functional domains. According to their specific epigenetic roles, they can be classified into three main categories: DNA methylases, histone modifying enzymes, and chromatin remodeling enzymes [20]. Accumulating evidence shows that the abnormal expressions of CRs were related to various biological processes, such as inflammation [21], autophagy [22], apoptosis [23], and proliferation [24], and the dysregulation of CR expression might contribute to various diseases. Thus, CRs could potentially serve as a novel target for the treatment of a variety of diseases. Importantly, a better understanding of CRs may be critical to understanding the progression of POAG as well as developing new treatments. However, no studies have systematically characterized the role of CRs in the pathogenesis of POAG. Thus, this research aims to establish a CR signature to provide new epigenetic insights into the pathogenesis of POAG.

2. Methods

2.1. Identification of differentially expressed CRs (DECRs)

The genome-wide expression profiles of human TM tissue between 13 controls and 15 POAG cases were obtained from the Gene Expression Omnibus database (GSE27276 [25], platform: GPL2507). In total, 870 CRs were retrieved from previous studies [19]. These genome-wide expression profiles were normalized through the "limma" R package. Based on the criteria of | logFC| >0.2 and false discovery rate (FDR) < 0.05, DECRs between the TM tissues of POAG patients and normal subjects were identified using the "limma" package based on R software (4.1.3). As such, the volcano map displayed them using the

"ggplot2" package. In addition, a heatmap was drawn using the "heatmap" package in R.

2.2. Functional enrichment analyses

Gene Ontology (GO) analysis (including molecular function (MF), biologic process (BP), and cellular components (CC)) of differentially expressed CRs was performed using the "ClusterProfiler" R package. The Kyoto Encyclopedia of Genes and Genomes (KEGG) pathway analysis was performed using the same approach as described previously. FDR and $p < 0.05$ were considered statistically significant. Furthermore, the Gene Set Enrichment analysis (GSEA) was conducted through the "ClusterProfiler" R package.

2.3. Protein-protein interaction (PPI) network construction and hub gene identification

The PPI network for DECRs was constructed using the Search Tool for the Retrieval of Interacting Genes (STRING) database (https://www.string-db.org). We chose the medium confidence (0.400) as the minimum required interaction score. CytoHubba plugin of Cytoscape software (3.6.1) was used to realize the visualization. In particular, the top 10 hub nodes of genes were selected by the Multiple Consensus Clustering (MCC) ranking degree method. Genes in the networks with the top 10 degrees in the PPI network were considered hub genes.

2.4. Immune signatures in POAG

The single-sample gene set enrichment analysis (ssGSEA) analysis was used to explore the correlation between CRs and infiltrating immune cells/immune functions, which was achieved through the "GSVA" R package [26]. Various markers for each type of immune cell and immune function were used. The marker genes for each immune cell population and immune function population were screened from previous studies. The ssGSEA enrichment scores obtained for each type of immune cell and immune function were then scaled and compared between the normal and POAG samples. The results were then demonstrated in boxplots using the "ggpubr" package. In addition, a heatmap was drawn using the "heatmap" R package. Next, the "corrplot" package was used to analyze the correlation between immune cells/ immune functions. The relationship between hub CRs and immune infiltration cells/immune functions was analyzed using the "psych" R package and "ggcorrplot" package and screened the hub genes that were most relevant to immunity; $p < 0.05$ was considered statistically significant.

2.5. Construction and evaluation of the nomogram

Firstly, the selected hub genes most relevant to immunity were used to construct the model and draw the nomogram. The "rms" R package drew the nomogram and the corresponding Calibration curve. In addition, the receiver operating characteristic (ROC) curve was drawn through the "ROCR"

R package. The Calibration curve and ROC curve were both used for model evaluation.

2.6. Co-expression analysis

Co-expression analysis was performed to identify the genes that had a co-expression relationship with the hub genes, and the filter condition was set to corFilter = 0.6 and pFilter = 0.001. The "circlize" package was used for visualization.

2.7. Gene set enrichment analysis (GSEA) analysis

The GSEA analysis was performed by the "Clusterprofiler" R package [27]. We downloaded two gene datasets ("c5.go.v7.4.symbols.gmt" and "c2.cp.kegg.v7.4.symbols.gmt") from the Molecular Signature Database (https://www.gsea-msigdb.org/gsea/msigdb/index.jsp) to act as reference gene sets for GO and KEGG analysis; $p < 0.05$ was considered to be statistically significant.

2.8. Construction of the miRNA-hub gene network

Enrichr (https://maayanlab.cloud/Enrichr/) predicted miRNAs associated with the selected hub genes. Cytoscape software (3.6.1) was used to construct the network map.

2.9. Identification of potential therapeutic agents for POAG

The selected hub genes most relevant to immunity were used to identify potential therapeutic agents for POAG. Enrichr (https://maayanlab.cloud/Enrichr/) was used for drug prediction. DSigDB database was used to obtain all possible candidate agents. The top 10 candidate agents were selected; $p < 0.05$ was considered statistically significant.

2.10. Culture of primary HTMCs

The remaining corneoscleral rings after corneal transplantation from non-glaucomatous cornea donors were collected, and the entire TM tissue was torn for primary cell culture. Primary HTMCs were cultured using the tissue mass culture method [28]. All tissue specimens were obtained in accordance with the Declaration of Helsinki. The Changsha Aier Eye Hospital eye bank provided tissue specimens. This study was approved by the ethics committee of Changsha Aier Eye Hospital (Ethics approval No. KYPJ0010). Cells were cultured in cell medium supplemented with 15% fetal bovine serum, 89% DMEM/F12, and 1% penicillin/streptomycin solution at 37°C in a 5% CO_2 incubator. The passage of any validated TM cells should be within 4–6 to retain the primary phenotypes.

30% Hydrogen peroxide (H_2O_2) was diluted to a specific concentration in a serum-free medium. After the appropriate time (1 h), the H_2O_2 intervention was stopped with twice phosphate-buffered saline (PBS) washing and further followed by Reactive oxygen species (ROS) reagent staining, Cell proliferation assays, or other functional assays.

2.11. Immunofluorescence staining

The HTMCs were fixed with methyl alcohol for 10 min and washed thrice with PBS at room temperature. Subsequently, the HTMCs were blocked in PBS containing 5% bovine serum albumin for 1 h at room temperature. After blocking, the HTMCs were incubated overnight in PBS containing primary antibodies at 4°C. The primary antibodies used were Collagen IV(COL-IV) and aquaporin 1(AQP1). Then, the cells were washed thrice with PBS again and incubated with secondary antibodies conjugated to Alexa Fluro 488 in PBS for 1 h at room temperature. After washing thrice with PBS, coverslips were mounted on slides using a mounting buffer containing DAPI for 5 min, and images were obtained using a Nikon fluorescence microscope.

2.12. Cell proliferation assays and lactate dehydrogenase (LDH) release test

A cell counting kit (CCK)-8 assay was performed to evaluate the cell proliferation capacity. HTMCs (4×10^3 per well) were seeded into 96-well plates. After 1 h of intervention (0.1 mm, 0.5 mm, 1 mm, 2 mm, 5 mm, 10 mm, 20 mm H_2O_2), 10% CCK8 was added to the cells. The optical density was then measured at 450 nm. Similarly, the LDH Cytotoxicity Assay Kit was used to evaluate cell cytotoxicity. The optical density was measured at 490 nm.

2.13. ROS detection test

ROS Assay Kit was used to explore intracellular ROS after treatment with H_2O_2 according to the manufacturer's instructions. Before loading the probe, the DCFH-DA probe was diluted with serum-free DMEM/F12 medium at a ratio of 1:1000 to reach a final concentration of 10 µmol/L. The H_2O_2 (0.5 mm 1 h) stimulated HTMCs were incubated with a DCFH-DA probe in the dark for 20 min. Finally, the green fluorescence was observed by a fluorescence microscope, and a multi-function microplate reader measured the fluorescence intensity.

2.14. RNA extraction and quantitative reverse-transcription polymerase chain reaction (qRT-PCR)

Total RNA was extracted using Trizol Reagent. After extraction, the RNA was first reverse-transcribed into cDNA. Genomic DNA was eliminated by treatment for 2 min at 42°C with 4×gDNA wiper Mix. Then, first-strand cDNA was synthesized using the 5×HiScript qRT SuperMixII. qRT-PCR for m6A-related genes was performed using ChamQ Universal SYBR qPCR Master Mix. The thermal conditions were as follows: initial denaturation at 95°C for 30 s, followed by 45 cycles of two-step amplification (95°C for 5 s, 60°C for 20s) and, finally, 95°C for 1 s, 65°C for 15s, and 95°C for 1 s for the dissociation curve. The relative fold changes of m6A-related genes were analyzed by the $2^{-\Delta\Delta Ct}$ method.

2.15. Statistics analysis

All bioinformatics analyses were conducted using R software (version 4.1.3). Data analysis was conducted by

GraphPad Prism (version 9.0). At least three biological and technical replicates of the cell experiments were performed. Continuous data are expressed as mean±standard deviation. Student's t-test and analysis of variance were used to examine the differences. Statistical significance was set at $p\text{-value} < 0.05$.

3. Results

3.1. Establishment and validation of CR-based signature

Aberrant expression of CRs has been implicated in the pathogenesis of many diseases, including cancer. Hence, it was interesting to analyze whether related changes could be detected in the TM tissues of POAG patients. Initially, the expression levels of these CRs [19] between human TM tissue of normal subjects and patients with POAG was scrutinized and compared. Data from 19 normal, 17 POAG samples of TM tissues were acquired from the Gene Expression Omnibus (GSE27276) database. These samples were then used to profile the expression of 870 CRs in POAG. The expression patterns of these CRs are shown in Figure 1(a). Compared with the normal TM tissues, 30 CRs, including 20 down-regulated CRs and 10 up-regulated CRs, were identified as DECRs (Figure 1(a,b)). This suggests their possible participation in the development of POAG.

Based on these DECRs, we performed GO and KEGG pathway functional enrichment analyses to explore the potential role of DECRs and related signaling pathways in POAG (Figure 1(c,d)). GO analysis showed that these DECRs were significantly enriched in BP terms, including histone modification, chromatin organization, response to steroid hormone, peptidyl-lysine modification, and hormone-mediated signaling pathway. Regarding CCs, these DECRs were mainly enriched in histone methyltransferase complex, methyltransferase complex, PcG protein complex, histone acetyltransferase complex, and protein acetyltransferase complex. Concerning MFs, these DECRs were primarily enriched in transcription coregulator activity, histone binding, chromatin DNA binding, histone demethylase activity, and protein demethylase activity. Moreover, KEGG analysis showed that these DECRs were mainly enriched in the MAPK signaling pathway.

Subsequently, the protein interactions of DECRs were analyzed through the STRING online database, and the PPI network was constructed (Figure 1(e)). CytoHubba was used to select the highly interacted genes, and the top 10 DECRs were obtained as the hub genes (Figure 1(f)). The obtained hub genes included lysine demethylase 5B (KDM5B), bromodomain and WD repeat domain containing 3 (BRWD3), histone deacetylase 8 (HDAC8), AT-rich interaction domain 2 (ARID2), MDS1 and EVI1 complex locus (MECOM), RB binding protein 7 (RBBP7), lysine demethylase 2A (KDM2A), chromobox 6 (CBX6), WD repeat domain 82 (WDR82) and PC4 and SRSF1 interacting protein 1 (PSIP1). Of them, WDR82, RBBP7, PSIP1, and CBX6 were up-regulated in POAG, whereas the others were down-regulated.
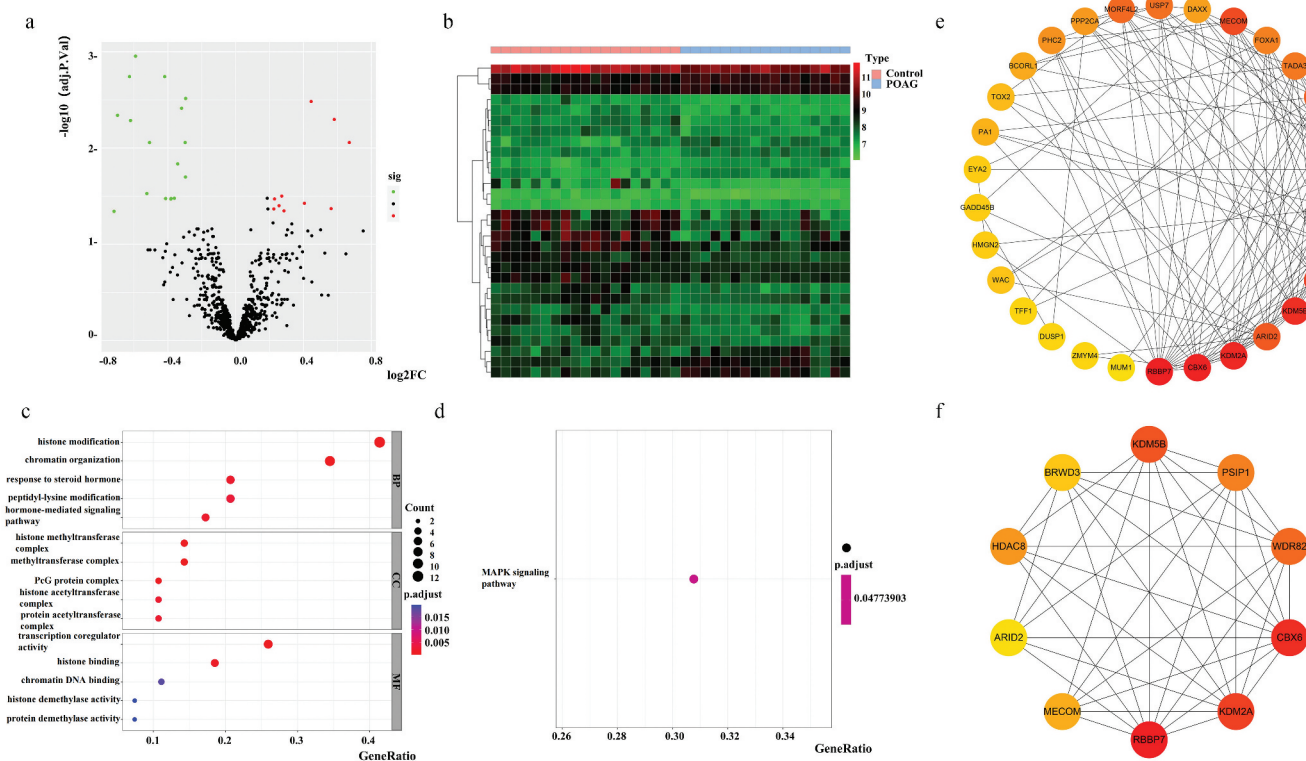

Figure 1. The expression landscape of 870 chromatin regulators (CRs) in POAG. (a) The volcano plot and (b) Heatmap of 30 differentially expressed CRs' expression among normal and primary open-angle glaucoma (POAG) samples. (a) Gene ontology (GO) enrichment analysis of the differentially expressed CRs. (c) GO and (d) Kyoto Encyclopedia of Genes and genomes (KEGG) enrichment analysis of the differentially expressed CRs. (e) Protein-protein interaction (PPI) network of differentially expressed CRs. (f) PPI network of the top 10 hub nodes of CRs.

3.2. Immune signatures in POAG

The immune microenvironment emerges as a critical player in the progression of diseases [29]. Clarifying the immune characteristics of TM tissue in POAG patients is helpful to enrich the exploration of the pathogenesis of POAG. We found that the dendritic cells (DCs), immature dendritic cells (iDCs), mast cells, follicular helper T (Tfh) cells, T helper 1 (Th1) cells, T helper 2 (Th2) cells, macrophages, neutrophils and Tumor Infiltrating Lymphocytes (TIL) components of POAG individuals were significantly different from normal controls from the perspective of the fold changes of immune cell components (Figure 2(a)). In addition, CC-chemokine receptor (CCR), Type II Interferon (IFN) Response, human leukocyte antigen (HLA), parainflammation, T cell co-stimulation, Type I IFN Response were different from the perspective of the fold changes of immune function components (Figure 2(b)). The above results suggested their possible participation in the development of POAG. The heatmap further showed the landscape of 16 kinds of immune cells and 13 kinds of immune function scores in POAG and non-glaucoma individuals (Figure 2(c)). Further, we performed the Spearman correlation analysis of the immune cells and the immune functions, respectively. As shown in Figure 2(d,e), the results of the correlation analyses were shown in red and blue, with red representing positive correlation and blue representing negative correlation. The results showed that the highest positive correlation coefficient in immune cells was detected between DCs and mast cells ($r =$ 0.6), and in immune functions, was detected between

checkpoint and T cell co-stimulation ($r = 0.81$). Meanwhile, the negative correlation coefficient in immune cells or immune functions was weak. Then, we also screened the hub genes that were most relevant to immunity and ended up with three genes, namely RBBP7, CBX6, and KDM5B (Figure 2(f)).

3.3. The generation and evaluation of nomogram based on the hub genes that were most relevant to immunity

As previously described, three hub genes were identified based on their association with immunity, namely RBBP7, CBX6, and KDM5B. The nomogram was drawn with these 3 CRs, as shown in Figure 3(a). The individual score of each gene can be obtained according to the expression levels of the 3 CRs in a patient. Then, the scores of all the CRs were added together to get a comprehensive score for the patient and realize the prediction of the risk of POAG. In addition, the model was evaluated using a calibration curve and ROC curve analysis (Figure 3(b,c)), which showed that the model had high accuracy (Area Under Curve (AUC) = 0.946). These results demonstrated the successful establishment of a nomogram based on CRs for predicting the risk of POAG.

3.4. Co-expression and GSEA analyses of the 3 hub CRs

Co-expression analyses were performed to identify the genes that had a co-expression relationship with the hub genes. The
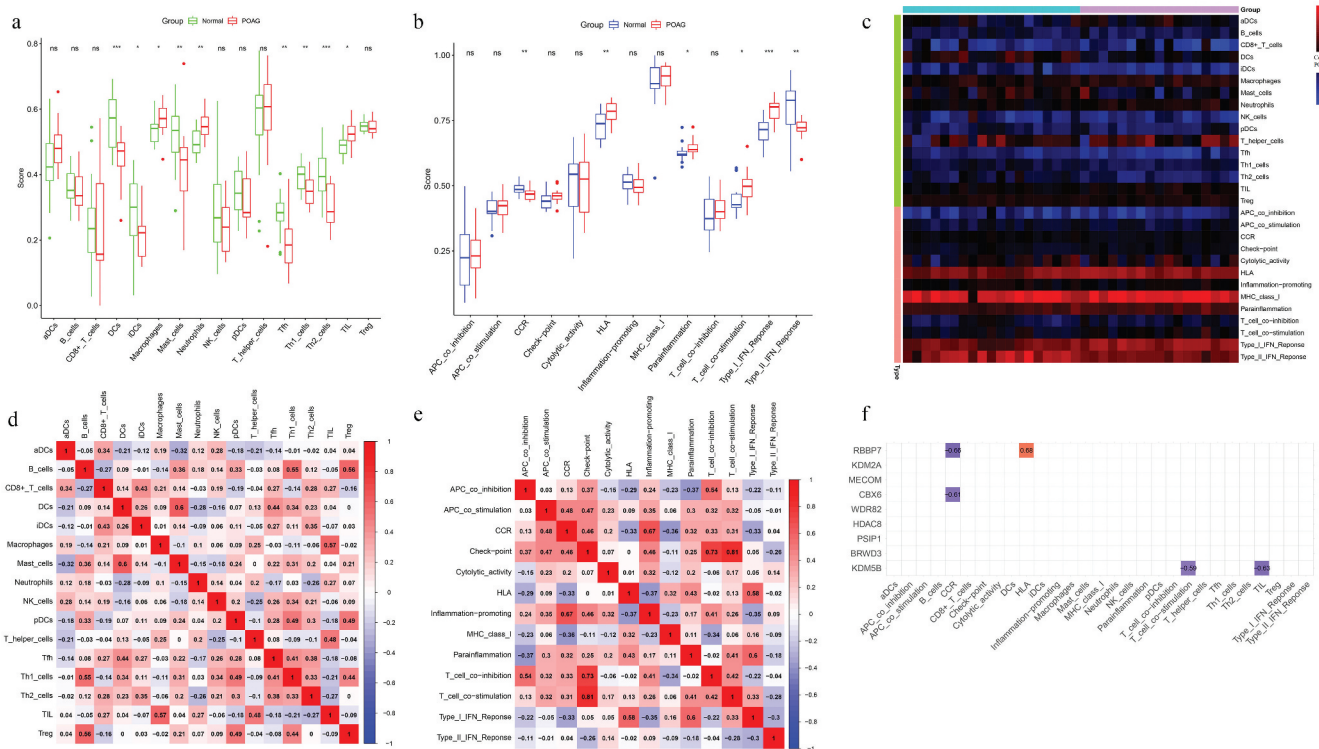

Figure 2. The immune signatures of POAG (a) Boxplots showing the infiltration of 8 kinds of immune cells with significant differences in trabecular meshwork (TM) between POAG and non-glaucoma individuals. (b) Boxplots showing significant differences in 6 immune function scores in TM between normal subjects and POAG patients. (c) The heatmap of 16 kinds of immune cells and 13 kinds of immune function scores in POAG and non-glaucoma individuals. (d) Spearman correlation analysis of 16 kinds of immune cell infiltration in TM of POAG patients. (e) Spearman correlation analysis of 13 kinds of immune function scores in TM of POAG patients. (f) The hub CRs most relevant to immunity. *$p < 0.05$; **$p < 0.01$; ***$p < 0.001$.
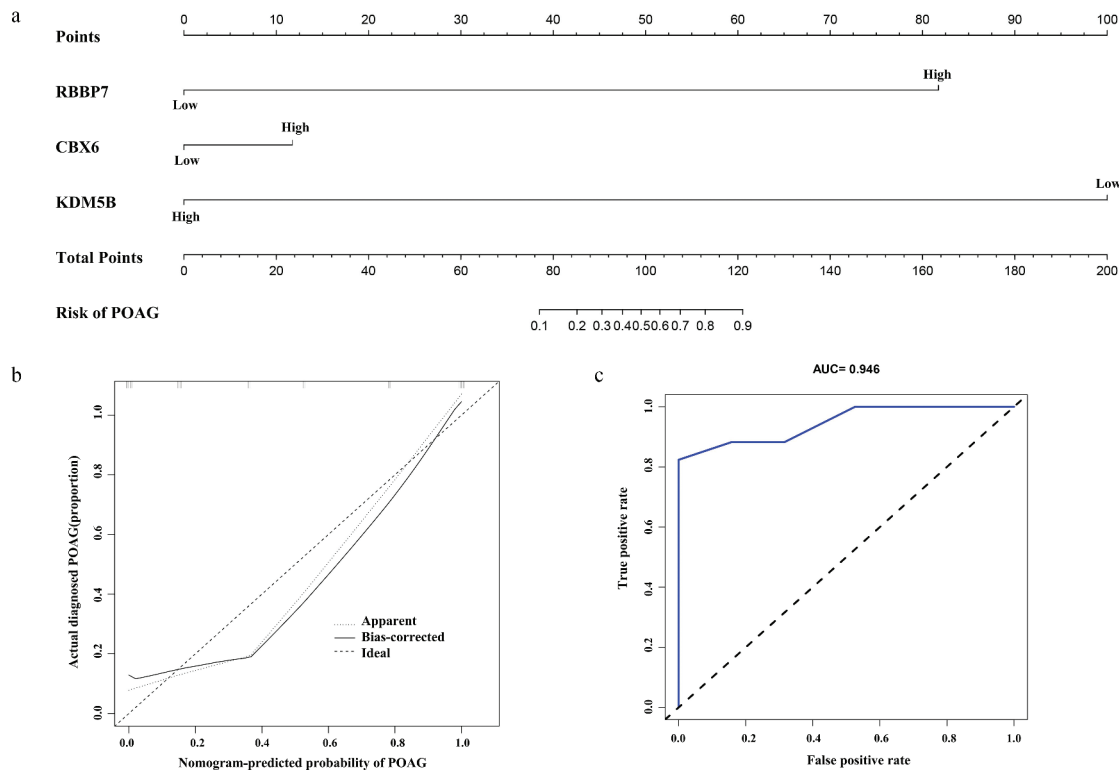
Figure 3. The generation and evaluation of a nomogram for predicting the risk of POAG based on CRs (a) Nomogram to estimate a patient's risk of developing POAG. (b) Calibration curve analysis and (c) Receiver operating characteristic (ROC) analysis show a high accuracy of the nomogram.

co-expression analysis results of the 3 hub CRs were shown in red and green lines. The top 10 genes whose expressions most correlated with 3 hub CRs expression were shown in (Figure 4 (a-c)). The color of the lines in the figure represented the degree of correlation, with green representing negative correlation and red representing positive correlation. The redder the line between two genes, the stronger the positive correlation between them. Similarly, the greener the line between two genes, the stronger the negative correlation between them. To further explore the molecular mechanisms of CR-based signatures, we performed GSEA analyses. The results indicated that KDM5B, CBX6, and RBBP7 were involved in similar human diseases, and all three were associated with Alzheimer's disease, Parkinson's disease, and Huntington's disease (Figure 4(g-i)). Oxidative phosphorylation was another pathway enriched in the high-expression group of KDM5B, CBX6, and RBBP7 (Figure 4(g-i)). In addition, the top 5 GO terms in each matrix were also displayed as classical GSEA graphs (Figure 4(d-f)).

3.5. miRNA-hub gene network construction

As a mode of epigenetics, miRNA plays an integral part in gene expression regulation. Based on the 3 hub CRs most associated with immunity, a miRNA-hub gene network containing 7 miRNAs was established (Supplementary Figure S1). The 7 hub miRNAs were miR-4484, miR-3147, miR-4750, miR-1258, miR-4278, miR-3117-3p and miR-1292.

3.6. Determine the CRs that might be involved in the regulation of cellular biological functions of HTMCs under oxidative stress

The corneal rings remaining after corneal transplantation from healthy corneal donors were collected, and TM tissues were isolated from the corneoscleral rims. The primary HTMCs were cultured by tissue mass culture method and were authenticated through AQP1 and COL-IV expression by cell immunofluorescence (Figure 5(a)). The HTMC oxidative stress cell model was constructed using H_2O_2 stimulation. Firstly, HTMCs were stimulated with different concentrations of H_2O_2 in vitro to induce oxidative stress. Cell viability examination showed that H_2O_2 treatment elicited a dose-dependent decline in HTMC viability, and treatment with 0.5 mm H_2O_2 for 1 h decreased cell viability to 68.85% ± 10.34%; cell viability was reduced to 9.08% ± 3.58% with 20 mm H_2O_2 for 1 h (Figure 5(b)). Cytotoxicity examination revealed that HTMC toxicity was increased by H_2O_2 treatment in the dose-dependent manner, and treatment with 0.5 mm H_2O_2 for 1 h increased cell toxicity to 36.05% ± 2.72%; cell toxicity was increased to 45.05%±0.86% with 20 mm H_2O_2 for 1 h (Figure 5(c)). To avoid H_2O_2 attenuation during the intervention process, we selected the intervention time of 1 h and an exposure concentration of 0.5 mm H_2O_2 as the optimal concentration for subsequent experiments. To observe the changes in intracellular ROS after treatment with 0.5 mm H_2O_2 for 1 h, the H_2O_2-stimulated HTMCs were incubated with a DCFH-DA probe. A fluorescence microscope observed the green fluorescence and the fluorescence intensity was measured by a multifunction microplate reader. It was found that the relative level of ROS increased from 1.00 ± 0.06 to 1.38 ± 0.19 (Figure 5(d,e)). It has
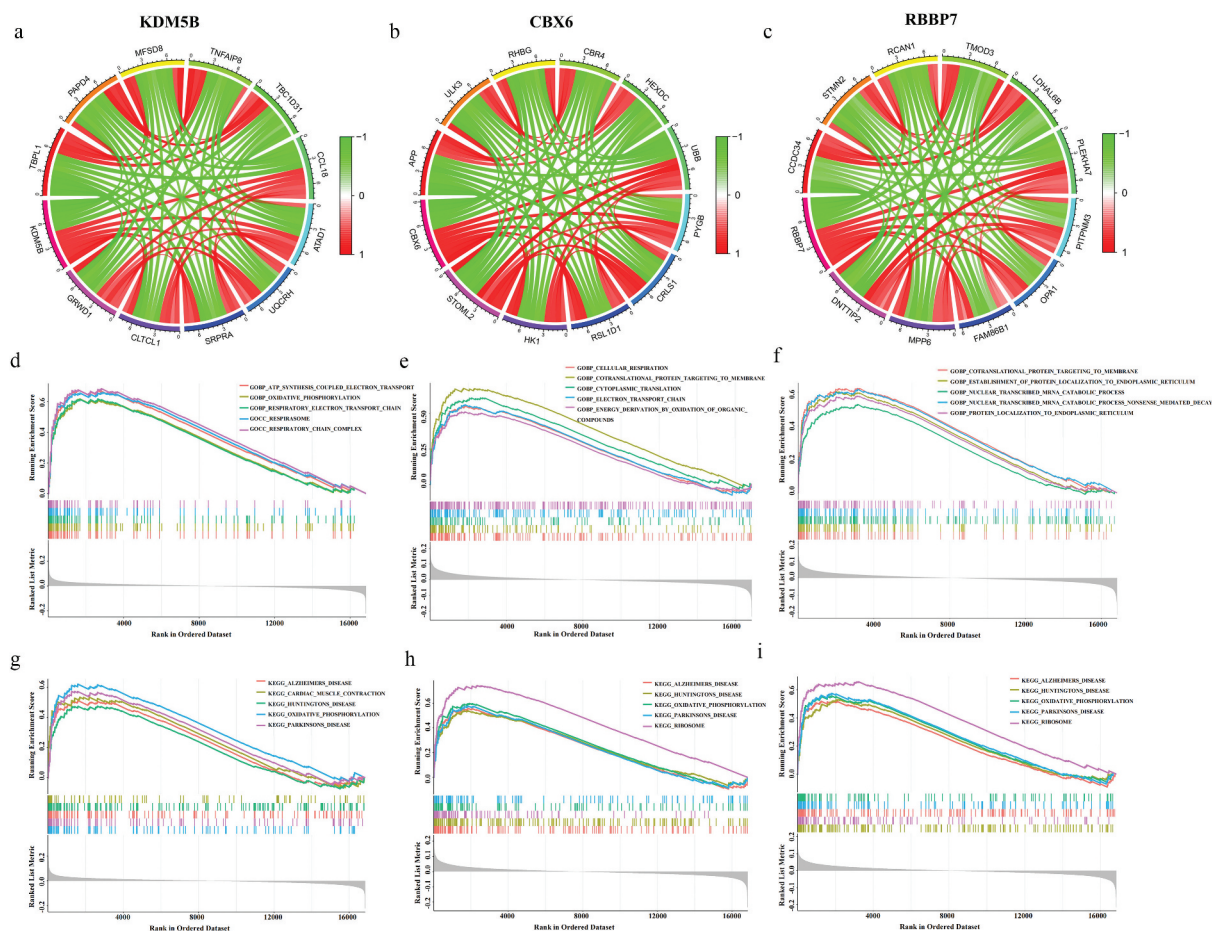
Figure 4. Co-expression and Gene set enrichment analysis (GSEA) of the 3 hub CRs. (a–c) identification of genes co-expressed with KDM5B/CBX6/RBBP7. (d–f) classical GSEA plots of the top 5 GO terms. (g–i) classical GSEA plots of the top 5 KEGG terms.

been proved that the method was feasible and that the model was established successfully. Next, the expression levels of the three differentially expressed CRs obtained by bioinformatics analyses were further verified in this model, and it was shown that the expression of KDM5B decreased significantly in the oxidative stress model (Figure 5(f)), which was consistent with the results of bioinformatics analyses.

3.7. Identification of potential therapeutic agents for POAG

Based on the expression of KDM5B, CBX6, and RBBP7, we also identified potential candidate agents for POAG, which might benefit the treatment of POAG. Compared with normal controls, the content of KDM5B, CBX6, and RBBP7 in TM tissues of POAG patients was different, and their expression levels were associated with immune status and had a good ability to predict the risk of POAG. Agents highly associated with KDM5B, CBX6, and RBBP7 might have potential therapeutic effects in POAG patients. Therefore, in this study, based on the expression of KDM5B, CBX6, and RBBP7 in TM tissues of POAG patients, we used the Enrichr website to do the analysis. The top 10 candidate agents were shown in Table 1, including Uranium acetate CTD 00000229, URANIUM CTD 00006964, fumonisin b1 CTD 00002395, 7646-79-9 CTD 00000928, METHOXYACETIC ACID

CTD 00000714, Promegestone CTD 00006626, hydrochloric acid, CTD 00006115, 8-azaguanine HL60 DOWN, syrosingopine PC3 UP and harmine PC3 UP. These compounds could be considered as potential therapeutic agents for POAG.

4. Discussion

Epigenetics is the study of some specific molecular mechanisms that cause heritable changes in gene expression or cell phenotype without changes in the DNA sequence. Numerous studies have elucidated its importance in the pathogenesis of disease. CRs are indispensable upstream regulators of epigenetics, which play a variety of functions in the occurrence of many diseases, such as tumors. However, to our knowledge, no studies have conducted a comprehensive analysis of CRs to explore the clinical significance of CRs in POAG.

We first screened 30 DECRs between the TM tissues of normal individuals and POAG patients in the GSE27276 database. We comprehensively explored the biological pathways of 30 CRs and constructed corresponding PPI networks. Then, we found that the immune microenvironment of the TM was changed in POAG patients, and we identified 3 CRs related to immunity. Based on the expression of 3 DECRs, we successfully established and validated a predicted signature, which could effectively predict the risk of POAG. Furthermore, the genes co-expressed with these 3 CRs and miRNAs with a regulatory
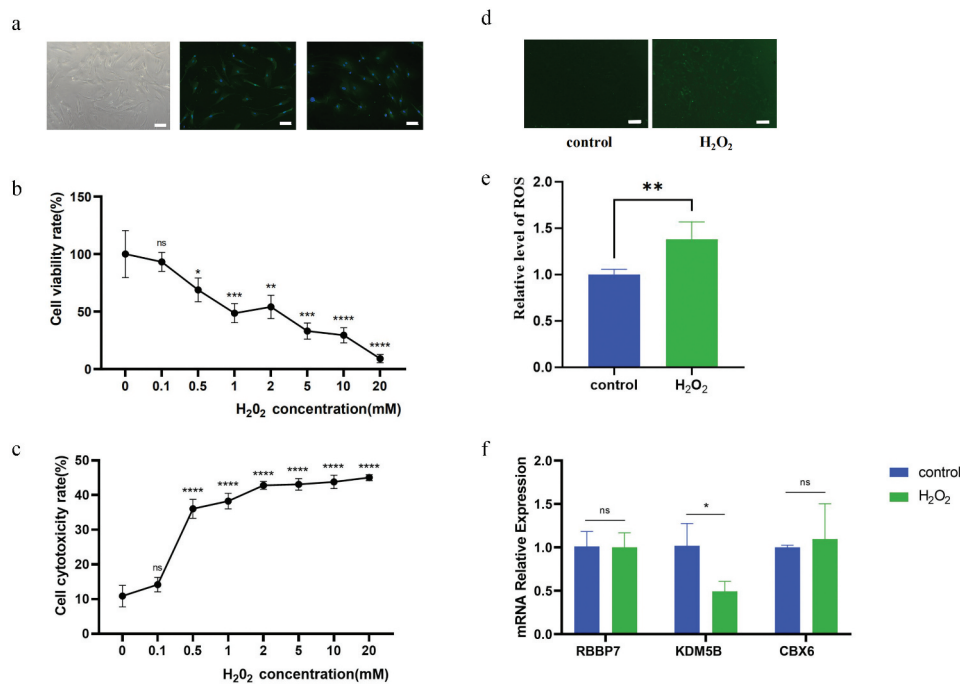
Figure 5. Establish the human trabecular meshwork cells (HTMCs) oxidative stress cell model and search for regulating CRs. (a) Culture and identification of primary HTMCs: HTMC cell morphology (Left); aquaporin 1 (AQP1) immunofluorescence staining (middle); collagen IV (COL-IV) immunofluorescence staining (right). (b) Cell counting kit (CCK)-8 was used to determine the proliferation of HTMCs treated with different concentrations of hydrogen peroxide(H_2O_2) for 1 h. (c) Lactate dehydrogenase (LDH) was used to assess the cytotoxicity of HTMCs treated with varying concentrations of H_2O_2 for 1 h. (d-e) the increase in reactive oxygen species (ROS) with H_2O_2 (0.5 mm)-treated HTMC over 60 min. Values in the plots are normalized against the control group. (f) Expression levels of three CRs in an oxidative stress cell model. $*p < 0.05$, $**p < 0.01$, $***p < 0.001$, $****p < 0.0001$ and ns, non-significant compared to the control group. Scale bar = 20 μm.

Table 1. Potential therapeutic agents of POAG.

Term	P-value	Genes
Uranium acetate CTD 00000229	4.38E−04	KDM5B;RBBP7
URANIUM CTD 00006964	4.48E−04	KDM5B;RBBP7
fumonisin b1 CTD 00002395	0.002248385	KDM5B
7646-79-9 CTD 00000928	0.003699205	KDM5B;CBX6;RBBP7
METHOXYACETIC ACID CTD 00000714	0.004792498	RBBP7
Promegestone CTD 00006626	0.004942017	RBBP7
hydrochloric acid CTD 00006115	0.005390484	KDM5B
8-azaguanine HL60 DOWN	0.005848207	CBX6;RBBP7
syrosingopine PC3 UP	0.009867756	KDM5B
harmine PC3 UP	0.010761596	CBX6

relationship with them were identified, and a miRNA-hub CR network was successfully constructed. It is worth mentioning that the GSEA analysis results showed that these 3 hub CRs were all associated with neurodegenerative diseases. In addition, we also found 10 agents that might be beneficial for the treatment of POAG patients.

GO analysis uncovered that the role of differentially expressed CRs included the regulation of DNA, histone, and chromatin. KEGG analysis indicated that 30 CRs were mainly involved in the MAPK signaling pathway. Substantial studies have shown that the MAPK signaling pathway is involved in the damage process of TM. Breedge et al. described changes in the transcriptome of normal primary TMCs induced by transforming growth factor-beta 2 (TGF-β2) using RNA-Seq and found that there is a change in MAPK signaling [30]. Chen et al. found that appropriate concentrations of TGF-β1 preserved TMCs from free radical-mediated damage by regulating p-AKT signaling balance and p-p38 MAPK level [31].

Meng et al. found thatσ-1 receptor stimulation prevented pressure-induced injury through insulin receptor-MAPK signaling in TMCs [32]. The above results indicated that CRs might play a role in developing POAG by regulating the MAPK signaling pathway.

The disorder of the immune microenvironment is an important factor in the occurrence of diseases [29]. CRs have been shown to function in physiological and pathological immune regulation [33,34]. Accumulating evidence has confirmed that TM interacts with the immune system in multiple ways. TM can participate in innate immune responses [35], be targeted by immune-mediated damage [36], undergo inflammation [37], and produce immunosuppressive factors [37]. Understanding these relationships is, therefore, helpful in revealing the complex mechanisms of diseases involving TM dysfunction. The immune characteristics were further explored to enrich the exploration of the pathogenesis of POAG. The results of ssGSEA showed differences in various immune cells and immune functions in the TM tissues of POAG patients. This suggested that there is a change in the immune status of the TM microenvironment in POAG, and the immune system disorders might play a critical role in the initiation and/or sustainment of glaucomatous TM damage. Notably, correlation analysis indicated that RBBP7, CBX6, and KDM5B might correlate with the immune response, suggesting that CRs might modulate the progression of POAG by regulating immune-infiltrating states. In addition, based on these 3 CRs, we successfully constructed a nomogram to predict the risk of POAG. Therefore, it is reasonable to consider that the dysregulation of CRs in TMCs of POAG patients indicates their

potential values as novel biomarkers for the diagnosis and targeted therapy of POAG.

KDM5B encodes a lysine-specific histone demethylase. Studies have shown that it plays a vital role in cell cycle regulation. Yang et al. found that KDM5B inhibited DNA damage and promoted the cell cycle in Granulosa cells, which might occur through the up-regulation of MTF1 [38]. It has also been shown that KDM5B licensed macrophage-mediated inflammatory responses by repressing Nfkbia transcription [39]. The CBX protein is a core component of polycomb repressive complex 1 and is involved in regulating the transcription process of polycomb proteins [40]. CBX6 is a member of the CBX family. Deng et al. proposed that CBX6 could inhibit the proliferation, migration, and invasion of human breast cancer cells [41]. Some researchers also proposed that knockdown of CBX6 promoted matrix metalloproteinase 2 (MMP-2) expression and invasion of mesothelioma cells [42]. RBBP7 is a ubiquitously expressed nuclear protein. Studies showed that RBBP7 was associated with the tumor immune response [43]. Wang et al. found that Hypoxia-induced HIF1α could promote the expression of cyclin-dependent kinase 4 by up-regulating the expression of RBBP7, thus increasing the viability, proliferation, and stemness of esophageal cancer cells [44]. Altogether, the three CRs are widely involved in various cellular functions and regulating inflammation and immunity. Therefore, we speculate that these hub CRs may also participate in the dysfunction of TM through the regulation of cellular functions and so on. It is worth mentioning that miRNAs play an essential role in the normal development of many biological processes as factors regulating gene expression. Many studies have shown that miRNAs play a key role in TM dysfunction in POAG patients [45,46]. MiRNAs can regulate the expression of CRs through post-transcriptional regulation [47], and CRs can also affect miRNA expression through epigenetic regulation such as chromatin remodeling [48]. A large number of studies have shown that miRNAs and CRs form a complex regulatory network to jointly regulate cellular processes, and their dynamic balance is crucial for maintaining cell homeostasis [49]. In this study, the construction of the miRNA-hub CR network established a link for the mutual molecular interactions between these three hub CRs and miRNAs. However, its specific regulatory effects and mechanisms still need further study.

Previous studies showed that oxidative stress, aging, genetics, and environmental and endogenous factors could cause TM damage. However, evidence from human and animal studies suggests that oxidative stress is considered a significant factor in such damage [50]. ROS are released after mitochondrial damage caused by various diseases, aging, oxidative stress, and other stress conditions [51]. Studies have confirmed that a large number of ROS exist in aqueous humor and TM of POAG patients, confirming their long-term exposure to oxidative stress [52]. Cellular or extracellular stimuli such as oxidative stress can cause damage to TM tissues, cause inflammation and death of HTMCs, thereby reducing aqueous humor drainage and causing increased IOP, eventually leading to glaucoma [53]. This study aims to explore the molecular mechanism of TM injury and HTMC death further to offer a novel understanding of the development of new therapeutic targets in POAG. To verify whether the three CRs previously screened play a role in TM damage, the HTMCs oxidative stress cell model commonly used in glaucoma studies was constructed. It is heartening that KDM5B was significantly down-regulated in this model. But there was no significant change in the expression levels of CBX6 and RBBP7. These results identified that KDM5B might be involved in cell damage during oxidative stress in the TM tissues. However, CBX6 and RBBP7 might have no biological role in this process, and there may be other biological mechanisms to be explored.

The results of GSEA analyses indicated that KDM5B, CBX6, and RBBP7 were involved in similar human diseases, and all three were associated with Alzheimer's disease, Parkinson's disease, and Huntington's disease. Intriguingly, all three diseases are neurodegenerative, and glaucoma is also considered a neurodegenerative disease. Multiple epidemiological studies suggest an association between POAG and major neurodegenerative disorders [54–57]. This is mainly because chronic, progressive loss of neurons is common in these diseases. Our result suggested that these three CRs might not only play a role in the disturbance of aqueous circulation caused by TM dysfunction in POAG patients but also might play an important role in optic nerve injury, and individuals with abnormal expression of these three genes might be more susceptible to POAG. Therefore, future clinical studies with a large sample size must elucidate these associations' biological nature. This might be a breakthrough in unraveling the relationship between POAG and degenerative diseases.

Finally, we used Enrichr website to predict the potential therapeutic agents and the top 10 candidate agents were selected, including Uranium acetate CTD 00000229, URANIUM CTD 00006964, fumonisin b1 CTD 00002395, 7646-79-9 CTD 00000928, METHOXYACETIC ACID CTD 00000714, Promegestone CTD 00006626, hydrochloric acid, CTD 00006115, 8-azaguanine HL60 DOWN, syrosingopine PC3 UP and harmine PC3 UP.

This study also has some shortcomings. The mechanisms of CRs regulating the biological behavior of TMCs need to be verified experimentally. In other words, key CRs need to be further explored, and their roles still need to be further verified by cell function experiments and animal experiments. The tissue specimens included in this study were obtained from African American and Caucasian donors. Our research group is collecting the TM tissues of the yellow race for further study to explore its general rule.

5. Conclusions

Dysregulation of CR expression in TM tissues may be involved in the occurrence and progression of POAG through multiple mechanisms. However, the exact mechanism still needs to be explored.

Author contributions

Xinyue Zhang and Lulu Xiao carried out the design of the idea of the article and was a major contributor in writing the manuscript; Xiaoyu Zhou, Jiahao Xu and Li Liao carried out the bioinformatic analysis; Ping Wu and Zhimin Liao assisted in the writing of the discussion section; Xuanchu Duan was responsible for the correction and revision of the manuscript; All authors read and approved the final manuscript.

Disclosure statement

Ethical declaration

This study was approved by the ethics committee of Changsha Aier Eye Hospital (Ethics approval No. KYPJ0010), and informed consent to participate was obtained from all of the participants.

Funding

Data availability statement

The sequencing data used in the paper came from the public database (GSE27276), and the additional experimental details and data are available from the corresponding author on reasonable request.

ORCID

Xuanchu Duan http://orcid.org/0000-0002-3148-1703

References

Papers of special note have been highlighted as either of interest (•) or of considerable interest (••) to readers.

1. Tham YC, Li X, Wong TY, et al. Global prevalence of glaucoma and projections of glaucoma burden through 2040: a systematic review and meta-analysis. Ophthalmology. 2014;121(11):2081–2090. doi: 10.1016/j.ophtha.2014.05.013
•• This paper is a summary of the current situation of glaucoma patients worldwide.
2. Bourne RRA, Flaxman SR, Braithwaite T, et al. Magnitude, temporal trends, and projections of the global prevalence of blindness and distance and near vision impairment: a systematic review and meta-analysis. Lancet Glob Health. 2017;5(9):e888–e97. doi: 10.1016/S2214-109X(17)30293-0
3. Rosenthal J, Leske MC. Open-angle glaucoma risk factors applied to clinical area. J Am Optom Assoc. 1980;51(11):1017–1024.
4. Buller C, Johnson DH, Tschumper RC. Human trabecular meshwork phagocytosis. Observations in an organ culture system. Invest Ophthalmol Vis Sci. 1990;31(10):2156–2163.
5. Alvarado J, Murphy C, Juster R. Trabecular meshwork cellularity in primary open-angle glaucoma and nonglaucomatous normals. Ophthalmology. 1984;91(6):564–579. doi: 10.1016/s0161-6420(84)34248-8
6. Alvarado J, Murphy C, Polansky J, et al. Age-related changes in trabecular meshwork cellularity. Invest Ophthalmol Vis Sci. 1981;21(5):714–727.
7. Liton PB, Challa P, Stinnett S, et al. Cellular senescence in the glaucomatous outflow pathway. Exp Gerontol. 2005;40(8–9):745––748. doi: 10.1016/j.exger.2005.06.005
8. Baleriola J, Garcia-Feijoo J, Martinez-de-la-Casa JM, et al. Apoptosis in the trabecular meshwork of glaucomatous patients. Mol Vis. 2008;14:1513–1516.
9. Hoare MJ, Grierson I, Brotchie D, et al. Cross-linked actin networks (CLANs) in the trabecular meshwork of the normal and glaucomatous human eye in situ. Invest Ophthalmol Vis Sci. 2009;50(3):1255–1263. doi: 10.1167/iovs.08-2706
10. Raghunathan V, Nartey A, Dhamodaran K, et al. Characterization of extracellular matrix deposited by segmental trabecular meshwork cells. Exp Eye Res. 2023;234:109605. doi: 10.1016/j.exer.2023.109605
11. Du Y, Yun H, Yang E, et al. Stem cells from trabecular meshwork home to TM tissue in vivo. Invest Ophthalmol Vis Sci. 2013;54(2):1450–1459. doi: 10.1167/iovs.12-11056
12. Gong G, Kosoko-Lasaki S, Haynatzki G, et al. Inherited, familial and sporadic primary open-angle glaucoma. J Natl Med Assoc. 2007;99(5):559–563.
13. Lee JS, Kuo CF, Chen WM, et al. Genetic and environmental contributions of primary angle-closure glaucoma and primary open-angle glaucoma: a nationwide study in Taiwan. Am J Ophthalmol. 2023;258:99–109. doi: 10.1016/j.ajo.2023.07.001
14. Wiggs JL. The cell and molecular biology of complex forms of glaucoma: updates on genetic, environmental, and epigenetic risk factors. Invest Ophthalmol Vis Sci. 2012;53(5):2467–2469. doi: 10.1167/iovs.12-9483e
15. Lu Y, Brommer B, Tian X, et al. Reprogramming to recover youthful epigenetic information and restore vision. Nature. 2020;588(7836):124–129. doi: 10.1038/s41586-020-2975-4
16. Zaidi SAH, Guzman W, Singh S, et al. Changes in class I and IIb HDACs by delta-opioid in chronic rat glaucoma Model. Invest Ophthalmol Vis Sci. 2020;61(14):4. doi: 10.1167/iovs.61.14.4
17. Gauthier AC, Liu J. Epigenetics and signaling pathways in glaucoma. Biomed Res Int. 2017;2017:5712341. doi: 10.1155/2017/5712341
18. Bermudez JY, Webber HC, Patel GC, et al. HDAC inhibitor-mediated epigenetic regulation of glaucoma-associated TGFbeta2 in the trabecular meshwork. Invest Ophthalmol Vis Sci. 2016;57(8):3698–3707. doi: 10.1167/iovs16-19446
19. Lu J, Xu J, Li J, et al. FACER: comprehensive molecular and functional characterization of epigenetic chromatin regulators. Nucleic Acids Res. 2018;46(19):10019–10033. doi: 10.1093/nar/gky679
20. Plass C, Pfister SM, Lindroth AM, et al. Mutations in regulators of the epigenome and their connections to global chromatin patterns in cancer. Nat Rev Genet. 2013;14(11):765–780. doi: 10.1038/nrg3554
21. Zhou Y, Sharma S, Sun X, et al. SMYD2 regulates vascular smooth muscle cell phenotypic switching and intimal hyperplasia via interaction with myocardin. Cell Mol Life Sci. 2023;80(9):264. doi: 10.1007/s00018-023-04883-9
22. Chen A, Zhou Y, Ren Y, et al. Ubiquitination of acetyltransferase Gcn5 contributes to fungal virulence in Fusarium graminearum. MBio. 2023:e0149923. doi: 10.1128/mbio.01499-23
23. Miura R, Mimura I, Saigusa H, et al. Chromatin remodeling factor, INO80, inhibits PMAIP1 in renal tubular cells via exchange of histone variant H2A.Z. For H2A. Sci Rep. 2023;13(1):13235. doi: 10.1038/s41598-023-40540-8
24. Liu Y, Yu K, Kong X, et al. FOXA1 O-GlcNAcylation-mediated transcriptional switch governs metastasis capacity in breast cancer. Sci Adv. 2023;9(33):eadg7112. doi: 10.1126/sciadv.adg7112

•• The sequencing results in the paper provided researchers with a lot of inspiration.

25. Liu Y, Allingham RR, Qin X, et al. Gene expression profile in human trabecular meshwork from patients with primary open-angle glaucoma. Invest Ophthalmol Vis Sci. 2013;54(9):6382–6389. doi: 10.1167/iovs.13-12128

26. Hanzelmann S, Castelo R, Guinney J. GSVA: gene set variation analysis for microarray and RNA-seq data. BMC Bioinformatics. 2013;14:7. doi: 10.1186/1471-2105-14-7

27. Yu G, Wang LG, Han Y, et al. clusterProfiler: an R package for comparing biological themes among gene clusters. OMICS. 2012;16(5):284–287. doi: 10.1089/omi.2011.0118

28. Keller KE, Bhattacharya SK, Borras T, et al. Consensus recommendations for trabecular meshwork cell isolation, characterization and culture. Exp Eye Res. 2018;171:164–173. doi: 10.1016/j.exer.2018.03.001

29. Makowski L, Chaib M, Rathmell JC. Immunometabolism: from basic mechanisms to translation. Immunol Rev. 2020;295(1):5–14. doi: 10.1111/imr.12858

30. Callaghan B, Lester K, Lane B, et al. Genome-wide transcriptome profiling of human trabecular meshwork cells treated with tgf-beta2. Sci Rep. 2022;12(1):9564. doi: 10.1038/s41598-022-13573-8

31. Chen HY, Chou HC, Ho YJ, et al. Characterization of TGF-β by induced oxidative stress in human trabecular meshwork cells. Antioxidants (Basel). 2021;10(1):107. doi: 10.3390/antiox10010107

32. Meng B, Li H, Sun X, et al. Sigma-1 receptor stimulation protects against pressure-induced damage through InsR-MAPK signaling in human trabecular meshwork cells. Mol Med Rep. 2017;16 (1):617–624. doi: 10.3892/mmr.2017.6647

33. Dong G, Wang Q, Wen M, et al. DDX18 drives tumor immune escape through transcription-activated STAT1 expression in pancreatic cancer. Oncogene. 2023;42(40):3000–3014. doi: 10.1038/s41388-023-02817-0

34. Meleady L, Towriss M, Kim J, et al. Histone deacetylase 3 regulates microglial function through histone deacetylation. Epigenetics. 2023;18(1):2241008. doi: 10.1080/15592294.2023.2241008

35. Sheng Q, Sun Y, Zhai R, et al. Murine cytomegalovirus localization and uveitic cell infiltration might both contribute to trabecular meshwork impairment in Posner-Schlossman syndrome: evidence from an open-angle rat model. Exp Eye Res. 2023;231:109477. doi: 10.1016/j.exer.2023.109477

36. Zhang D, Wu J, Zhang S, et al. Identification of immune infiltration-related ceRNAs as novel biomarkers for prognosis of patients with primary open-angle glaucoma. Front Genet. 2022;13:838220. doi: 10.3389/fgene.2022.838220

37. Yarishkin O, Phuong TTT, Vazquez-Chona F, et al. Emergent temporal signaling in human trabecular meshwork cells: role of TRPV4-TRPM4 interactions. Front Immunol. 2022;13:805076. doi: 10.3389/fimmu.2022.805076

38. Yang Y, Cai Y, Guo J, et al. Knockdown of KDM5B leads to DNA damage and cell cycle arrest in granulosa cells via MTF1. Curr Issues Mol Biol. 2023;45(4):3219–3237. doi: 10.3390/cimb45040210

39. Zhang Y, Gao Y, Jiang Y, et al. Histone demethylase KDM5B licenses macrophage-mediated inflammatory responses by repressing nfkbia transcription. Cell Death Differ. 2023;30(5):1279–1292. doi: 10.1038/s41418-023-01136-x

40. Bernstein BE, Mikkelsen TS, Xie X, et al. A bivalent chromatin structure marks key developmental genes in embryonic stem cells. Cell. 2006;125(2):315–326. doi: 10.1016/j.cell.2006.02.041

41. Deng H, Guan X, Gong L, et al. CBX6 is negatively regulated by EZH2 and plays a potential tumor suppressor role in breast cancer. Sci Rep. 2019;9(1):197. doi: 10.1038/s41598-018-36560-4

42. Sakai K, Nishiuchi T, Tange S, et al. Proteasomal degradation of polycomb-group protein CBX6 confers MMP-2 expression essential for mesothelioma invasion. Sci Rep. 2020;10(1):16678. doi: 10.1038/s41598-020-72448-y

43. Wang H, Lu X, Chen J. Construction and experimental validation of an acetylation-related gene signature to evaluate the recurrence and immunotherapeutic response in early-stage lung adenocarcinoma. BMC Med Genomics. 2022;15(1):254. doi: 10.1186/s12920-022-01413-7

44. Wang R, Huang Z, Lin Z, et al. Hypoxia-induced RBBP7 promotes esophagus cancer progression by inducing CDK4 expression. Acta Biochim Biophys Sin (Shanghai). 2022;54(2):179–186. doi: 10.3724/abbs.2021027

45. Zhou X, Zhang F, Zhang X, et al. Construction of miRNA-mRNA regulatory network indicates potential biomarkers for primary open-angle glaucoma. BMC Med Genomics. 2023;16(1):280. doi: 10.1186/s12920-023-01698-2

46. Doyle C, Callaghan B, Roodnat AW, et al. The TGFβ induced MicroRNAome of the trabecular meshwork. Cells. 2024;13 (12):1060. doi: 10.3390/cells13121060

47. Varambally S, Cao Q, Mani RS, et al. Genomic loss of microRNA-101 leads to overexpression of histone methyltransferase EZH2 in cancer. Science. 2008;322(5908):1695–1699. doi: 10.1126/science.1165395

48. Zhang X, Zhao X, Fiskus W, et al. Coordinated silencing of myc-mediated miR-29 by HDAC3 and EZH2 as a therapeutic target of histone modification in aggressive B-Cell lymphomas. Cancer Cell. 2012;22(4):506–523. doi: 10.1016/j.ccr.2012.09.003

49. Gu H, Chen Q, Li J. The MiR-101/EZH2 negative feedback signaling drives oxygen-glucose deprivation/reperfusion-induced injury by activating the MAPK14 signaling pathway in SH-SY5Y cells. Acta Biochim Pol. 2022;69(2):437–446. doi: 10.18388/abp.2020_5921

50. Welge-Lussen U, Birke K. Oxidative stress in the trabecular meshwork of POAG. Klin Monbl Augenheilkd. 2010;227(2):99–107. doi: 10.1055/s-0029-1245171

51. Rahal A, Kumar A, Singh V, et al. Oxidative stress, prooxidants, and antioxidants: the interplay. Biomed Res Int. 2014;2014:761264. doi: 10.1155/2014/761264

52. Fan Y, Guo L, Wei J, et al. Effects of Salidroside on trabecular meshwork cell extracellular matrix expression and mouse intraocular pressure. Invest Ophthalmol Vis Sci. 2019;60(6):2072–2082. doi: 10.1167/iovs.19-26585

53. Sacca SC, Gandolfi S, Bagnis A, et al. From DNA damage to functional changes of the trabecular meshwork in aging and glaucoma. Ageing Res Rev. 2016;29:26–41. doi: 10.1016/j.arr.2016.05.012

54. Jain S, Aref AA. Senile dementia and glaucoma: evidence for a common link. J Ophthalmic Vis Res. 2015;10(2):178–183. doi: 10.4103/2008-322X.163766

55. Matlach J, Wagner M, Malzahn U, et al. Retinal changes in Parkinson's disease and glaucoma. Parkinsonism Relat Disord. 2018;56:41–46. doi: 10.1016/j.parkreldis.2018.06.016

56. Carreras FJ. Glaucoma and amyotrophic lateral sclerosis, two kindred diseases? Neural Regen Res. 2016;11(9):1415–1417. doi: 10.4103/1673-5374.191211

57. Chan JW, Chan NCY, Sadun AA. Glaucoma as neurodegeneration in the brain. Eye Brain. 2021;13:21–28. doi: 10.2147/EB.S293765